



Application of crossplot and prestack seismic-based impedance inversion for discrimination of lithofacies and fluid prediction in an old producing field, Eastern Niger Delta Basin

C. G. Okeugo¹ · K. M. Onuoha¹ · C. A. Ekwe² · O. A. Anyiam¹ · C. I. P. Dim¹

Received: 17 November 2017 / Accepted: 10 June 2018 / Published online: 21 June 2018
© The Author(s) 2018

Abstract

Lithofacies distributions and continuity are very important for proper reservoir development; and predicting the fluid types will also help in reducing uncertainties associated with characterizing hydrocarbon reservoirs. This study used Poisson impedance attributes and crossplots from prestack seismic inversion and well logs to discriminate and predict hydrocarbon-filled reservoirs in the Bumma Field, Greater Ughelli Depobelt, Niger Delta Basin. Seismic inversion and well log data were integrated to image and characterize lithofacies at reservoir zones of interest. A supervised model-based simultaneous inversion of Poisson impedance (PI) and crossplot was carried out on the prestack seismic data to understand the lithofacies classification and fluid types. Four classifications of lithofacies (clean sand, sandyshale, shaly-sand and shale) were discriminated based on the well log crossplot between gamma ray and Poisson impedance. The sand lithofacies shows low values of gamma ray (< 65 API) and PI (< -100 ft/s*g/cc) while shale lithofacies possesses high values of gamma ray (> 65 API) and PI (> -100 ft/s*g/cc). Also, well log and inverted results from PI showed that values with less than -100 ft/s*g/cc represent hydrocarbon-filled sand, whereas greater values represent brine and shale. These classifications provide better decision in predicting and discriminating lithofacies accurately. Furthermore, generated map revealed the presence of hydrocarbon-filled reservoirs in a northeast–southwest trending meandering channel. The successful application of crossplot and seismic-based impedance inversion will be helpful in discriminating lithofacies and predicts fluids for accurate location of new wells for optimum production from the field.

Keywords Acoustic impedance · Cross-plot · Lithofacies · Poisson impedance · Prestack seismic data · Simultaneous inversion

Introduction

In the Niger Delta basin, the search for more hydrocarbons has, with time, shifted from onshore to near shelf and now to the deep water. Although, it is believed that the high cost of operations in deep water environments, followed by inability to characterize lithofacies and predict fluid types accurately across the basin depobelts are few major factors to contend with. Generally, the prediction of lithofacies

and fluid type have over the years pose great challenge to reservoir geologists and geophysicists working on the old producing fields (discovered in the late 1950s with oil production from 1961) in onshore Niger Delta basin. Although, recent advances in seismic technology have led to development of methods such as Poisson impedance (PI) inversion, lambda–mu–rho inversion, elastic impedance inversion, EI and rock physics template modelling, and RPT to help characterize lithofacies and predict fluid types (Coulon et al. 2006; Singh et al. 2007; Ekwe et al. 2012; Tian et al. 2010; Sharma and Chopra 2013; Farfour et al. 2015; Tucovic et al. 2016). Advances on the use of prestack migrated seismic (PreSTM) data have tremendously helped in characterizing lithofacies and predicting reservoir properties with minimum error thereby reducing the numbers of dry wells and drilling risks in some basins of the world (Ma 2002; Russell 2014). Characterizing lithofacies and predicting fluid types from

✉ C. G. Okeugo
chukwudike.okeugo@unn.edu.ng

¹ Department of Geology, University of Nigeria, Nsukka, Nigeria

² Department of Geology and Geophysics, Federal University Ndufu-Alike Ikwo, Ikwo, Nigeria

the Niger Delta basin using prestack migrated seismic data and well logs requires great skill and better understanding of seismic inversion techniques. Numerous studies have been conducted on the use of different seismic inversion types to characterize lithology and predict fluid types in Niger Delta basin. Most of the studies focused on the use of simultaneous, deterministic and geostatistical inversion to construct reliable earth and petrophysical models (Omodu et al. 2007; Ujuanbi et al. 2008; Nwogbo et al. 2009). One main advantage of using prestack seismic inversion for constructing reliable earth model and characterizing lithofacies is based on the ability of the technique to extract more information (such as shear velocity, Vs) from seismic data to better discriminate reservoir and non-reservoir rocks that are not answered by poststack seismic inversion.

The study area falls within the southern part of the Bumma Field (Fig. 1), which Reijers (2011) reported as being shalier than the northern part of the field, thus having lower chances of productive reservoirs. Shell Petroleum Development Company Internal Report, (2007) highlighted that the lack of productive reservoirs in the southern part of the field have significantly led to drilling marginal and dry wells (Table 1), so there is need to adopt an improved technique such as cross-plot analysis of Poisson impedance

Table 1 Wells showing status of production in the selected area of study

Well name	Spud date	Status
AG	1974	Dry
AG-002XX	1974	Dry
AB	1961	Oil/gas
A	1992	Oil/gas
B	1965	Oil/gas
C	1989	Gas
AW-00XX	1980	Marginal
NKIX-001XX	1977	Marginal
ALB-001XX	1965	Marginal

and its inversion to discriminate lithofacies and predict fluid types in Bumma Field. The Poisson impedance was first published by Quakenbush et al. (2006) and they derived the attribute seismically by combining the discrimination characteristics of Poisson’s ratio along with density, both of which are parameters useful in reservoir delineation. Also, several works have highlighted Poisson impedance as a very favorable attribute for identifying new prospect and characterizing clastic reservoir (Mazumdar 2007; Omodu

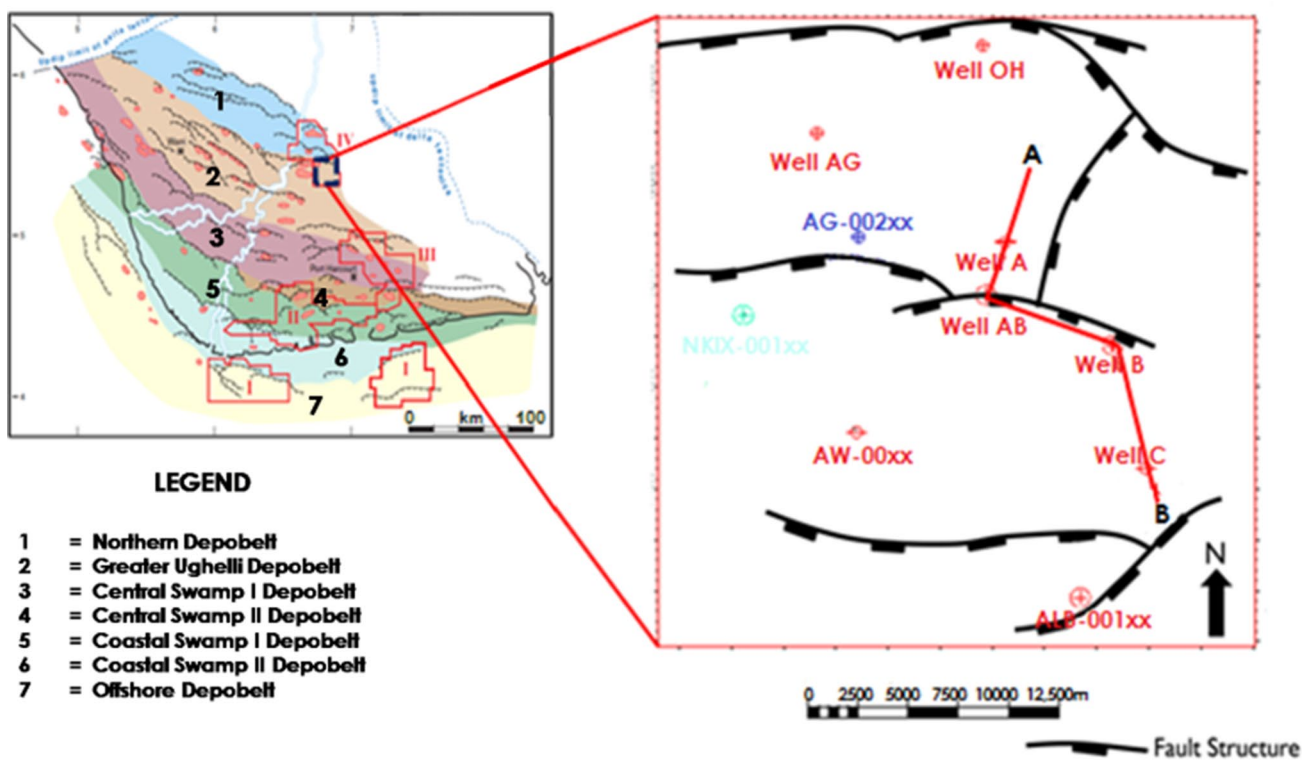


Fig. 1 A Niger Delta view showing position of Bumma Field, well positions, correlation line across major fault system between northern (a) and southern (b) parts of the field

et al. 2007; Tian et al. 2010; Zhou and Hilterman 2010; and; Sharma and Chopra 2013). Therefore, the main aim of this study is to use cross-plot analysis and seismic simultaneous inversion-derived Poisson impedance to discriminate lithofacies and predict fluid types associated with H-reservoirs (comprising of H1, H4 and H5 sands) in Bumma Field.

Geologic background

Bumma field is located in the Greater Ughelli Depobelt of the onshore Niger Delta basin. The stratal package within the study area is formed from a major regressive cycle that resulted in deposition of allocyclic units of transgressive marine sand, marine shale, shoreface and fluvial back swamp deposits (Reijers 2011). The three lithostratigraphic units in the study area are from the bottom: the pro-delta facies of Akata Formation, paralic delta front facies of Agbada Formation and continental facies of Benin Formation (Fig. 2a). The Akata Formation is the oldest of the three formations with age ranging from Eocene to recent (Reijers et al. 2011; Lawrence et al. 2002). They are deep marine shale and serve as source rock (Short and Stauble 1967). The Akata shales formed during the early development stages of Niger Delta progradation and are typically under-compacted and over-pressured. The shales also form diapiric structures including shale swells and ridges which often intrude into overlying Agbada Formation (Fig. 2b). It is exposed in the inland, north-eastern part of Niger Delta as the Imo shale. The Benin Formation is the youngest and comprises the top part of the Niger Delta clastic wedge, from the Benin–Onitsha area in the north to beyond the coast line (Short and Stauble 1967). The Agbada Formation overlies the Akata Formation and constitutes the main reservoir and seal for hydrocarbons accumulation in the Niger Delta. The formation occurs throughout Niger Delta clastic wedge and has a maximum thickness of about 13,000 feet (Doust and Omatsola 1989). The lithologies consist of alternating sands, silts and shales, arranged within 10–100 feet successions, and defined by progressive upward changes in grain size and bed thickness. The strata are generally interpreted to have been formed in fluvial–deltaic environment. The top of the formation is recent, and its base extends to a depth of 4600 feet. The base is defined by the youngest marine shale. Shallow parts of the formation are composed entirely of non-marine sand deposited in alluvial or upper coastal plain environments during progradation of the delta (Doust and Omatsola 1989).

The structural and stratigraphic settings of the field are mainly controlled by pre- and syn-sedimentary tectonic elements that responded to variable rates of subsidence and sediment supply during Late Eocene to Oligocene times (Doust and Omatsola 1990; Reijers 2011). Structurally, the macrostructures found in the area, according to Evamy et al.

(1978); Stacher (1995); Reijers (2011), range from simple rollover anticlines, multiple growth faults, antithetic faults and collapsed crest faults (Fig. 2c) with most of these faults offsetting at different parts of the Agbada Formation and flattening into Eocene detachment planes near the top of the Akata Formation (Reijers et al. 1997).

The stratigraphic setting, according to Orife and Avbovbo (1981); Petters (1984); SPDC Internal Report (2007) witnessed the cutting of Opuama Channel into the Orogbo megasequence (34.4 Ma) in the western part of the delta leading to channel formation in the northern section of the active Greater Ughelli Depo-belt as a result of sea level fall at 35.4 Ma. Locally, the sequences deposited are characterized by proximal deltaic deposits and channel units that are separated by laterally extensive shale packages that represent flooding episodes, as shown in Fig. 3.

Materials and methodology

Available dataset used for this study include a full 3-D Pre-stack Time Migration (PreSTM) seismic volume and suites of wire line log comprising gamma ray, density–neutron, resistivity, shear and compressional velocity from nine wells as shown in Table 2. The PreSTM seismic volume and three wells (A, C and AG-002XX) were quality-checked (QC) and prepared for seismic simultaneous inversion process, before loading them into the Hampson Russell CE8R4.4.1 software. Essential log data required for the inversion workflow (Fig. 4) are P-wave sonic, S-wave sonic, density and check shots logs.

Theoretical background

Prestack seismic simultaneous inversion

Prestack seismic inversion is a stratigraphic deconvolution technique that has, over the last couple of years, been used for reservoir characterization due to its sensitivity to resolve thin-bed tuning for increased stratigraphic resolution in many cases (Duboz et al. 1998; Veeken and Silva 2004). The primary aim of this inversion technique is to obtain reliable estimates of acoustic impedance (Z_p), shear impedance (Z_s), compressional velocity and shear velocity ratio, V_p/V_s and Poisson ratios attributes from reflection amplitude, travel time and waveform data at non-normal incidence for more robust interpretation of lithology and fluid content (Ma 2002; Hampson et al. 2005; Sen 2006). The estimations of these attributes are based on the relations of the incident, reflected, and transmitted longitudinal waves and shear waves on both sides of a plane interface (Singleton 2011), and this has been discussed by several authors; for instance Ma (2002) and (Sen 2006) highlighted that the

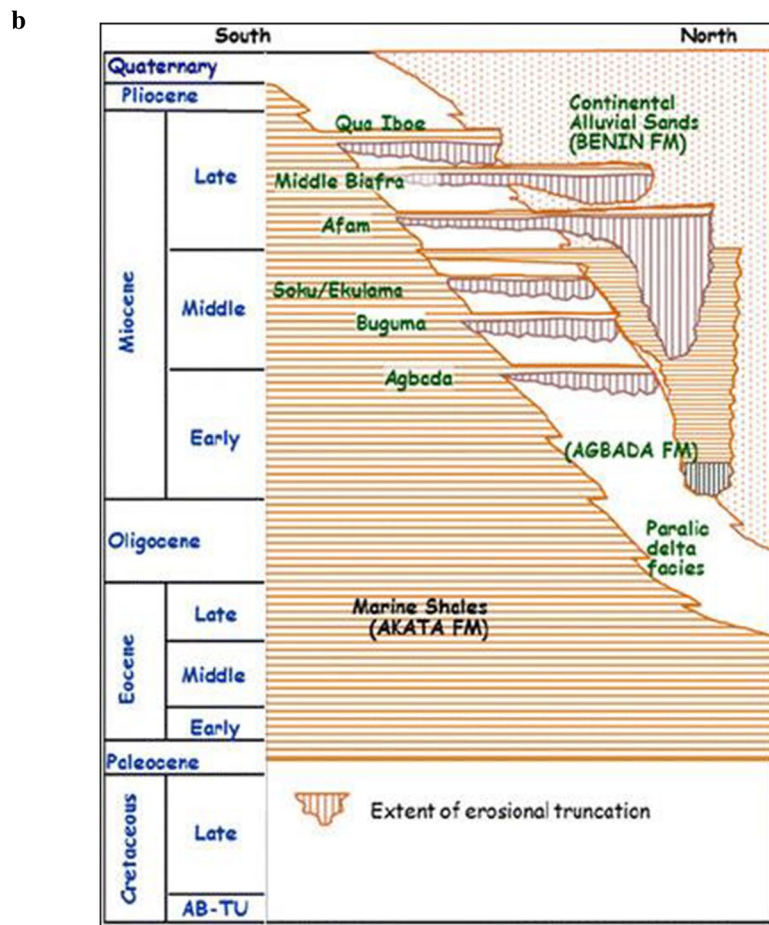
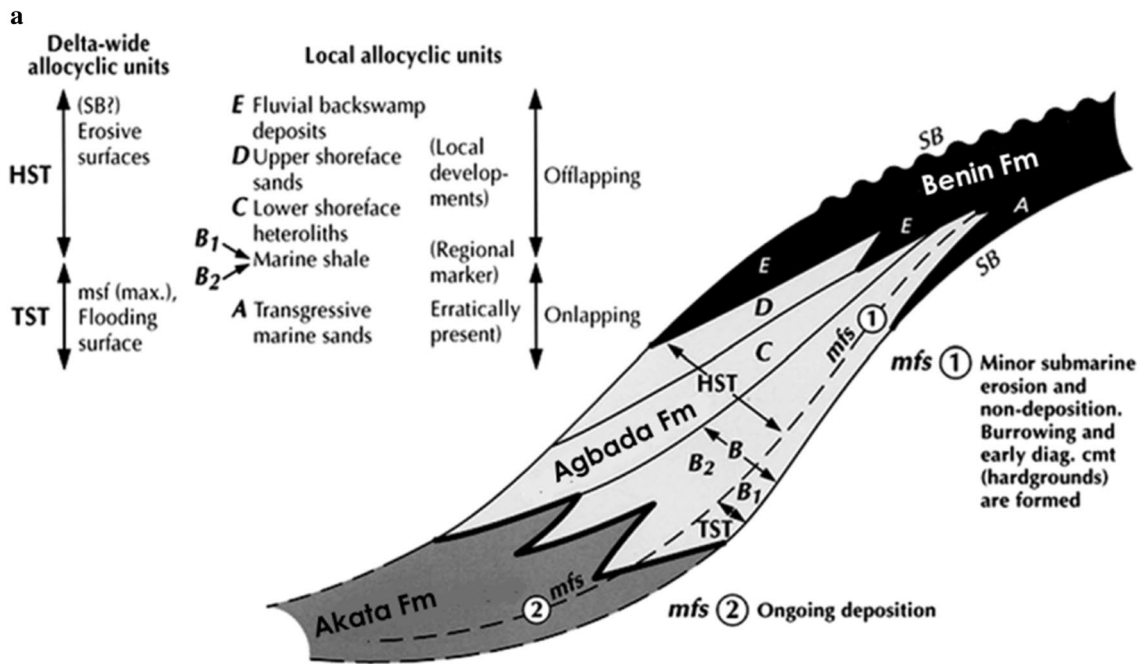


Fig. 2 a Schematic diagram showing the three alloctyclic units of the three formations (adopted from Reijers 2011). **b** Stratigraphy of the Niger Delta showing the lithologic units of the three formations

(adopted from Lawrence et al. 2002). **c** Generalized dip section of the Niger Delta showing the structural provinces of the Delta (adopted from Whiteman 1982)

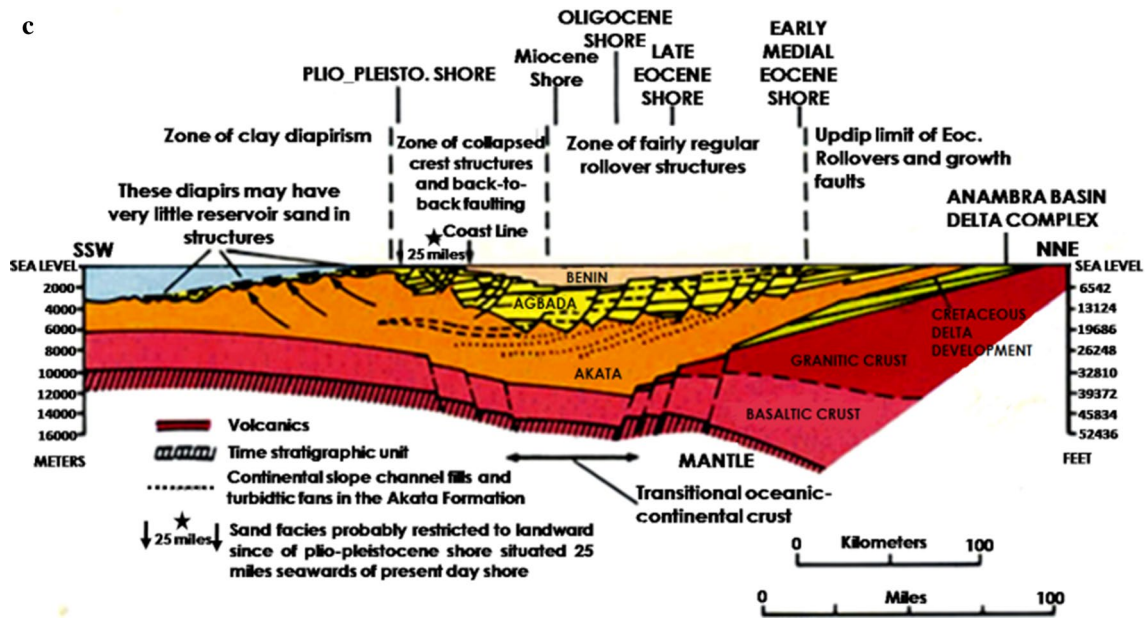


Fig. 2 (continued)

Zoeppritz equations are used to describe the relations of incident, reflected, and transmitted longitudinal waves and shearwaves on both sides of a plane interface. This first-order approximation to reflectivity (Zoeppritz equations) is given by Aki and Richards (1980) equation as an approximate relationship between the P-wave reflection coefficient $R(\theta)$ and the angle of incidence θ as follows:

$$R(\theta) \approx \frac{1}{2} \left(\frac{\Delta V_p}{V_p} + \frac{\Delta \rho}{\rho} \right) - 2 \left(\frac{V_s}{V_p} \right)^2 \left(2 \frac{\Delta V_s}{V_s} + \frac{\Delta \rho}{\rho} \right) \times \sin^2 \theta + \frac{1}{2} \frac{\Delta V_p}{V_p} \tan^2 \theta \quad (1)$$

where V_p is the average P-wave velocity between two uniform half-spaces, V_s is the average S-wave velocity, and ρ is the average density. The assumptions following the approximations are (1) that the relative changes of property ($\Delta V_p/V_p$, $\Delta V_s/V_s$, and $\Delta \rho/\rho$) are small, (2) that the second-order terms can be neglected, and (3) that θ is much less than 90° . Therefore, Eq. (1) can be rewritten in terms of P-wave and S-wave impedances as:

$$R(\theta) \approx (1 + \tan^2 \theta) \frac{\Delta Z_p}{2Z_p} - 8 \left(\frac{V_s}{V_p} \right)^2 \sin^2 \theta \frac{\Delta Z_s}{2Z_s} - \left[\tan^2 \theta - 4 \left(\frac{V_s}{V_p} \right)^2 \sin^2 \theta \right] \frac{\Delta \rho}{2\rho} \quad (2)$$

where $Z_p = V_p \rho$ is the average acoustic impedance, $Z_s = V_s \rho$ is the average shear impedance, $\Delta Z_p/2Z_p = 1/2(\Delta V_p/V_p) + \Delta \rho/\rho$ is the zero-offset P-wave reflection coefficient, and $\Delta Z_s/2Z_s = 1/2(\Delta V_s/V_s) + \Delta \rho/\rho$ is the zero-offset S-wave reflection coefficient. Later, Fatti et al. (1994) simplified the P-wave reflection coefficient $R(\theta)$ by assuming that the third term in Eq. (2) involving ρ , only cancels for most V_s/V_p ratios around 0.5 and small angles, and simplified the Zoeppritz's equations as:

$$R(\theta) \approx (1 + \tan^2 \theta) \frac{\Delta Z_p}{2Z_p} - 8 \left(\frac{V_s}{V_p} \right)^2 \sin^2 \theta \frac{\Delta Z_s}{2Z_s} \quad (3)$$

This approximation has been used over time to extract the P- and S-impedance reflectivities by fitting the P-wave reflection amplitudes from CMP gathers. It is also believed that the background (V_s/V_p) ratio must be known a priori, else P- and S-impedance reflectivity could produce a biased or physically unreasonable solution (Wang 1999). To overcome this limitation, Ma (2002) replaced (V_s/V_p) by (Z_s/Z_p) , such that the reflection coefficients $R(\theta)$ are only a function of only three parameters: Z_p , Z_s and θ . Equation 3 then becomes,

$$R(\theta) \approx (1 + \tan^2 \theta) \frac{\Delta Z_p}{2Z_p} - 8 \left(\frac{Z_s}{Z_p} \right)^2 \sin^2 \theta \frac{\Delta Z_s}{2Z_s} \quad (4)$$

These forms the basis of a simultaneous inversion procedure that estimates acoustic and shear impedances (Z_p and Z_s)

Fig. 3 Lithologic sequence from well A in northern part of the Bumma field. (31.3MFS, 32.4SB, 33.0MFS, 33.3SB, and c34.4_MFS are the maximum flooding surfaces and sequence boundaries defined over the Oligocene sequence)

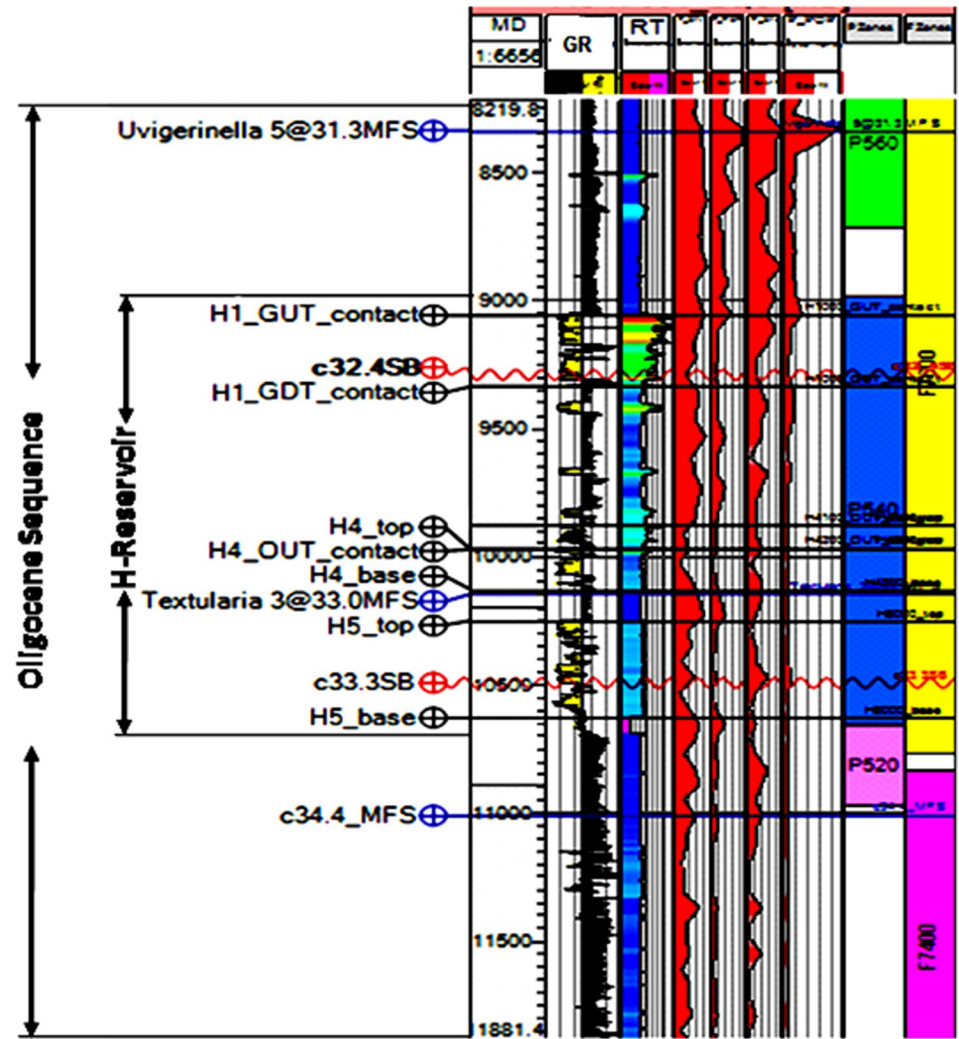
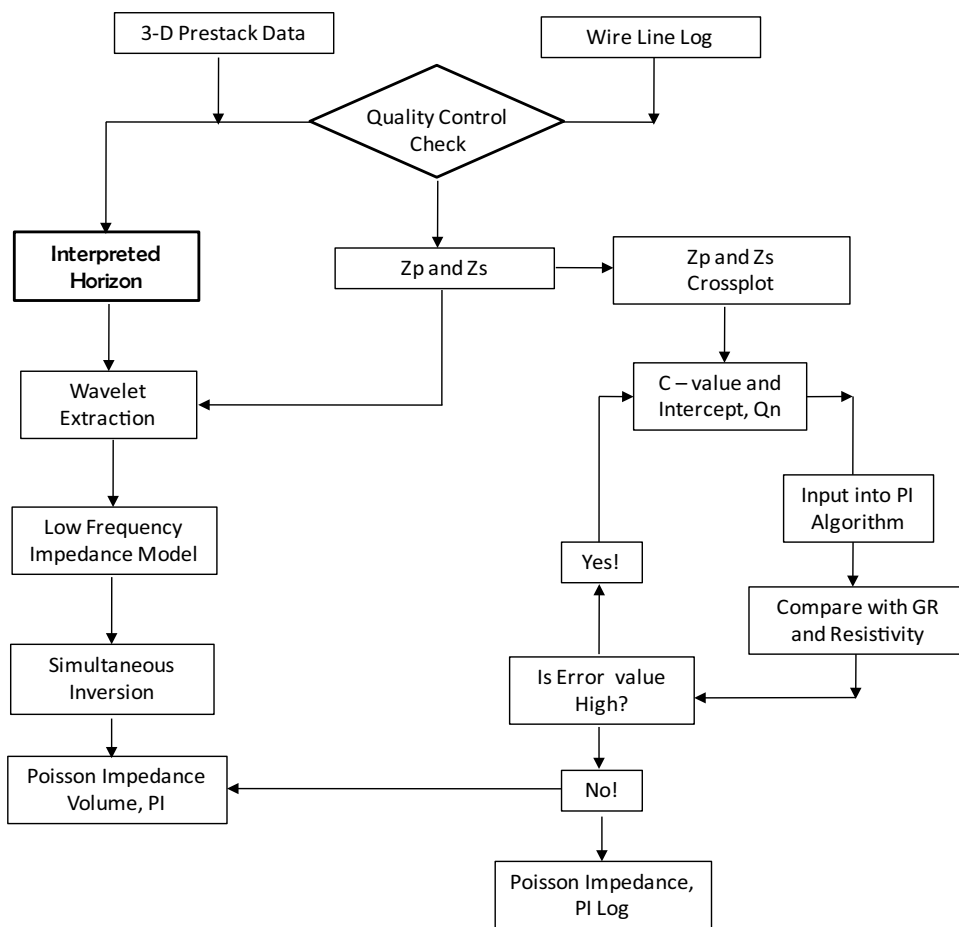


Table 2 Data quality chat from wells in BUMMA Field

Well name	Lithologic logs		Resistivity log			Density	Neutron	Compress- sional sonic	Shear sonic
	SP	GR	SN	ILD	LLD				
AG	Yes	Yes	No	No	Yes	Yes	No	Yes	No
AG-002XX	Yes	Yes	No	No	Yes	Yes	Yes	Yes	Yes
AB	Yes	Yes	Yes	No	Yes	No	No	Yes	No
A	No	Yes	Yes	No	Yes	Yes	Yes	Yes	Yes
B	Yes	Yes	Yes	Yes	Yes	No	Yes	Yes	No
C	Yes	Yes	Yes	Yes	Yes	Yes	Yes	Yes	Yes
AW-00XX	No	Yes	Yes	Yes	Yes	Yes	Yes	No	No
NKIX-001XX	NA	NA	NA	NA	NA	NA	NA	NA	NA
ALB-001XX	No	Yes	Yes	No	Yes	No	No	Yes	No

Fig. 4 Schematic workflow of model-based simultaneous inversion for Poisson impedance extraction by combined use of seismic and well log data



from prestack seismic gathers. The basic assumptions made from the approximation (Eq. 4) are that the earth has approximately horizontal layers at each common depth point and that each layer is described by both acoustic and shear impedances. Once acoustic impedance Z_p and shear impedance Z_s volumes have been created, they can be easily used to create other useful volumes, such as Poisson impedance, PI and lambda-rho, $\lambda\rho$ and mu-rho, $\mu\rho$, which are the product of density and the Lamé elastic constants λ and μ (Goodway et al. 1997).

Poisson impedance attribute (log and seismic)

Poisson impedance is a relatively novel attribute and sensitivity tool developed for discriminating lithology and fluid content (Quakenbush et al. 2006). The Poisson impedance attribute is a set of combined impedances (acoustic and shear) that are optimized by axis rotation to produce better resolution of lithology and fluid content (Quakenbush et al. 2006 and; Sharma and Chopra 2013). The attribute has showed many successful applications in delineating hydrocarbon-filled and brine-filled sands from shales (Mazumdar 2007; Omudu et al. 2007; Zhou and Hilterman 2010; Tian

et al. 2010; and; Nair et al. 2012). The mathematical Poisson impedance is defined as,

$$PI(t) = Z_p(t) - C_n * Z_s(t) + Q_n = Z_p(t) - \left[\frac{Z_p}{Z_s} \right]_{\text{wet}} Z_s(t) + Q_n \quad (5)$$

where $Z_p(t)$ = Acoustic Impedance trace, (ft/s)(g/cc)

where $Z_s(t)$ = Shear Impedance trace, (ft/s)(g/cc)

C_n or $\left[\frac{Z_p}{Z_s} \right]_{\text{wet}}$ = Rotation optimization Factor

(Generated from the slope of the $Z_p(t)$ – $Z_s(t)$ crossplot)

Q_n = Intercept value at $Z_p(t)$ axis

$PI(t)$ = Poisson Impedance, (ft/s)(g/cc)

The lithology optimization factor C_n and Intercept Q_n were determined as slope and intercept values of the crossplot regression line between acoustic and shear impedance from well A which is the control well (Fig. 5). Generation of Poisson Impedance from well log as shown in Fig. 6a requires an input of the C_n , Q_n and acoustic impedance

(Z_p) and shear impedance (Z_s) into Eq. 5. Crossplot analysis between Poisson impedance with gamma ray log was also determined using well A to help understand lithofacies distribution with respect to classifying them as clean sand, sandy-shale, shaly-sand and shales at inter-well distances (Fig. 6b).

On seismic, Poisson impedance attribute was generated following seismic simultaneous inversion steps, which require independent volumes of acoustic impedance (Z_p) trace, and shear impedance (Z_s) trace. A zero-phased wavelet was extracted statistically from two wells (A and C) following the calibration of well to seismic as shown in Fig. 7a. Total of four horizons or reflection events (31.3MFS, 32.4SB, 33.0MFS and c34.4MFS) were picked as maximum flooding surfaces (MFS) and sequence boundary (SB) for the seismic inversion. Picked reflection events are based on the reversed polarity convention, which defines the peak as a decrease in acoustic impedance and trough as increase in acoustic impedance with depth (Fig. 7b). A low frequency model representing acoustic and shear impedances and density was generated to accurately perform inversion analysis as shown in Fig. 8. The main outputs of the inversion analysis are the inverted volumes of acoustic impedance (Z_p) and shear impedance (Z_s), which are inputted into the Eq. 5 for generation of Poisson impedance, PI volume (Fig. 9).

Results and discussion

Lithofacies discrimination from Poisson impedance log

Lithofacies discrimination using Poisson Impedance was designed to correlate with gamma ray signatures for better reservoir resolution. Results based on lithology cut-off

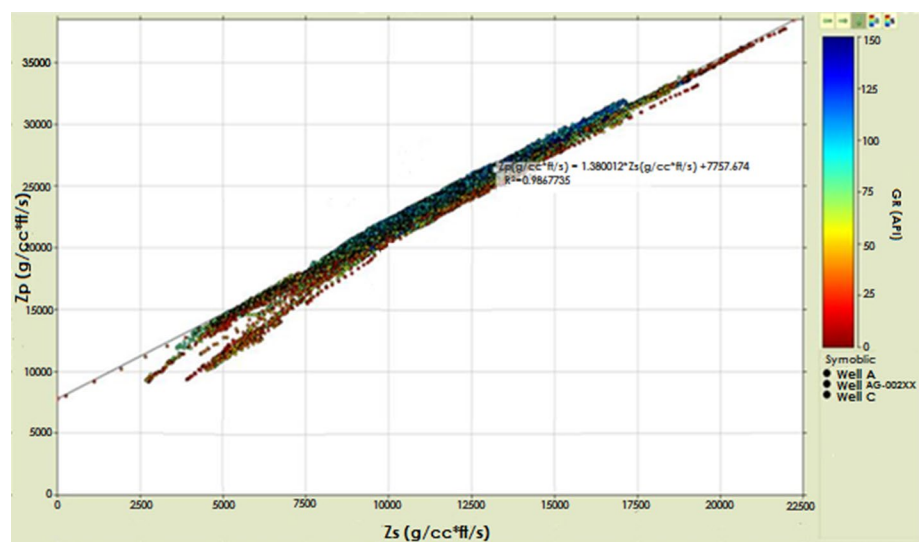
Fig. 6 a Log section showing lithofacies similarities between measured gamma ray log and Poisson impedance log of well A. Note: sand facies are represented by yellow color while shale facies are gray color. **b** Lithology discrimination chart between Poisson impedance and gamma ray log showing distributions of various lithofacies

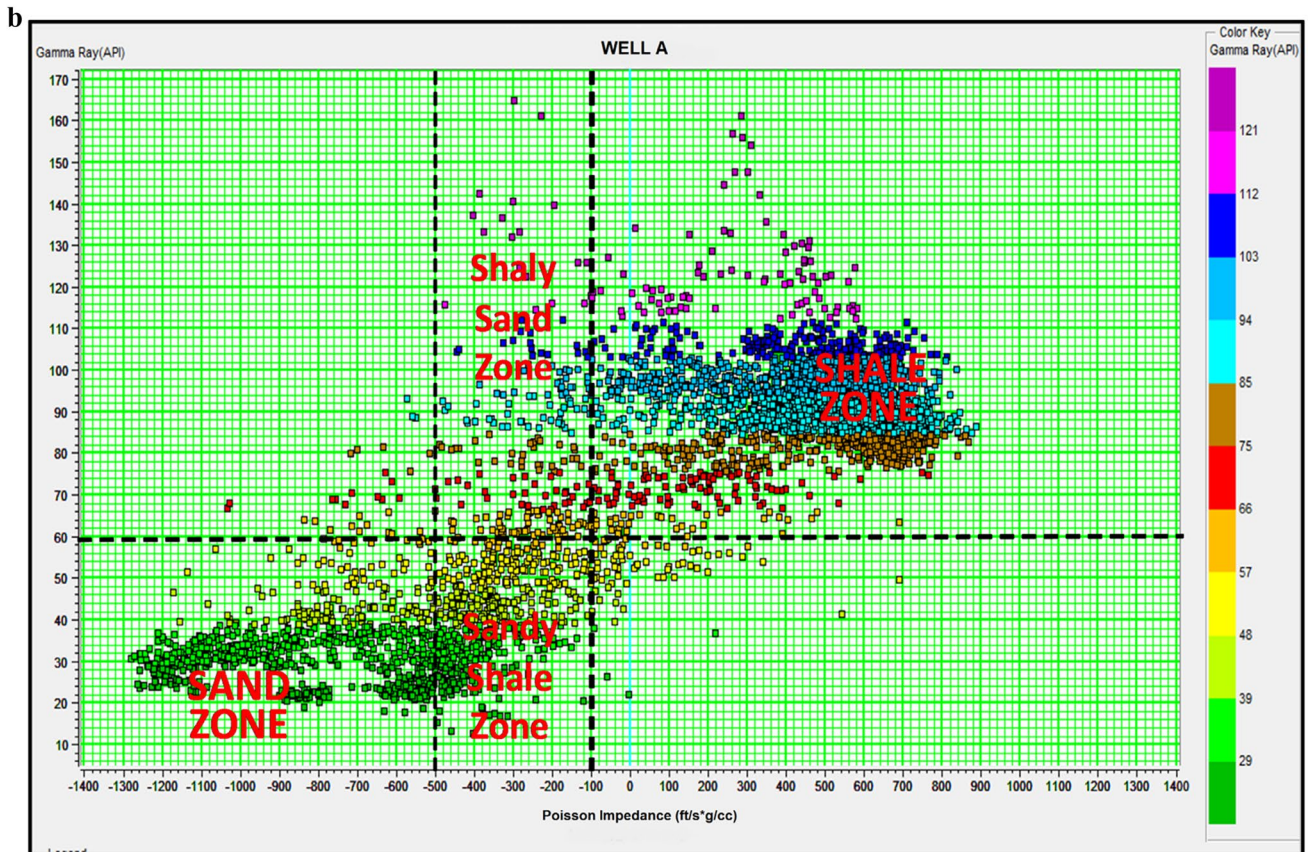
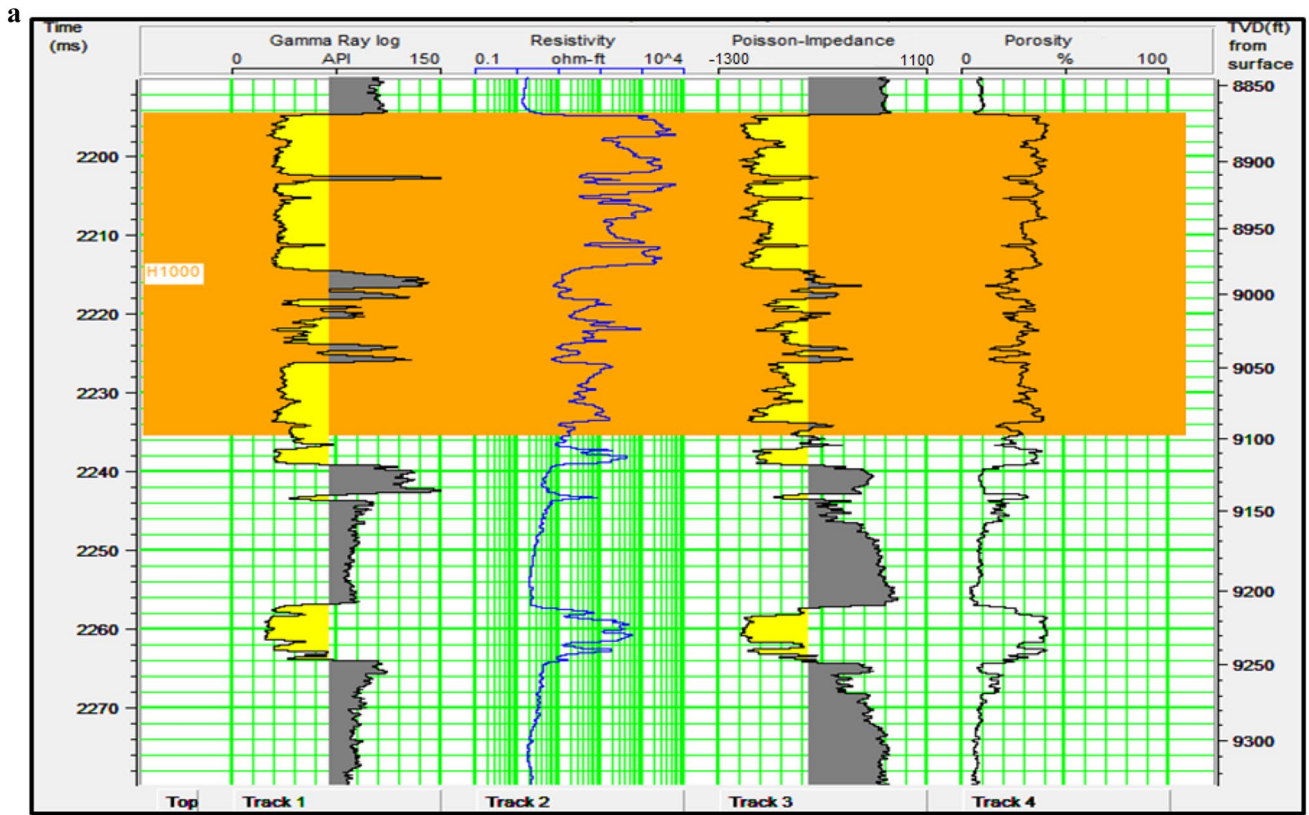
shows that gamma ray and Poisson impedance values less than 65 API and $-100 \text{ ft/s}^* \text{g/cc}$ represent sand, while values greater than 65API and $-100 \text{ ft/s}^* \text{g/cc}$ represent shale (Fig. 6a). Well log correlation between Poisson impedance and gamma ray logs over high resistive zones ensure higher confidence in the discrimination and prediction lithofacies and fluid types. Two major lithofacies (sand and shale) and two heteroliths (sandy-shale and shaly-sand) were identified based on Poisson impedance log cross-plot with gamma ray, as shown in Fig. 6b. The validation of Poisson Impedance and gamma ray signatures showed good correlation as lithofacies from well A confirmed that both signatures reflect same as comprising of shales with associated coarsening upward regressive sequence (Fig. 6a).

Lithofacies discrimination and fluid prediction from Poisson impedance inversion

Successful discrimination of lithofacies from seismic data requires good estimation of seismic wavelet (amplitude and phase spectra) and seismic synthetic to properly fit and calibrate major time events on both log and seismic. Extracted wavelet was observed to be symmetrical with a maximum at time zero (Fig. 7b); this wavelet shape was very useful for increased resolving power and ease of picking reflection events (peak or trough) for seismic scaling and modeling purpose, especially at deeper sections of the seismic. Analysis of the inversion parameters from wells A and C showed that there are some mismatches in the initial and

Fig. 5 Cross-plot of Z_p verses Z_s from three wells used to generate rotation optimization factor, C_n and intercept Q_n (1.380012 and 7757.674). Insert: Color code is gamma ray values





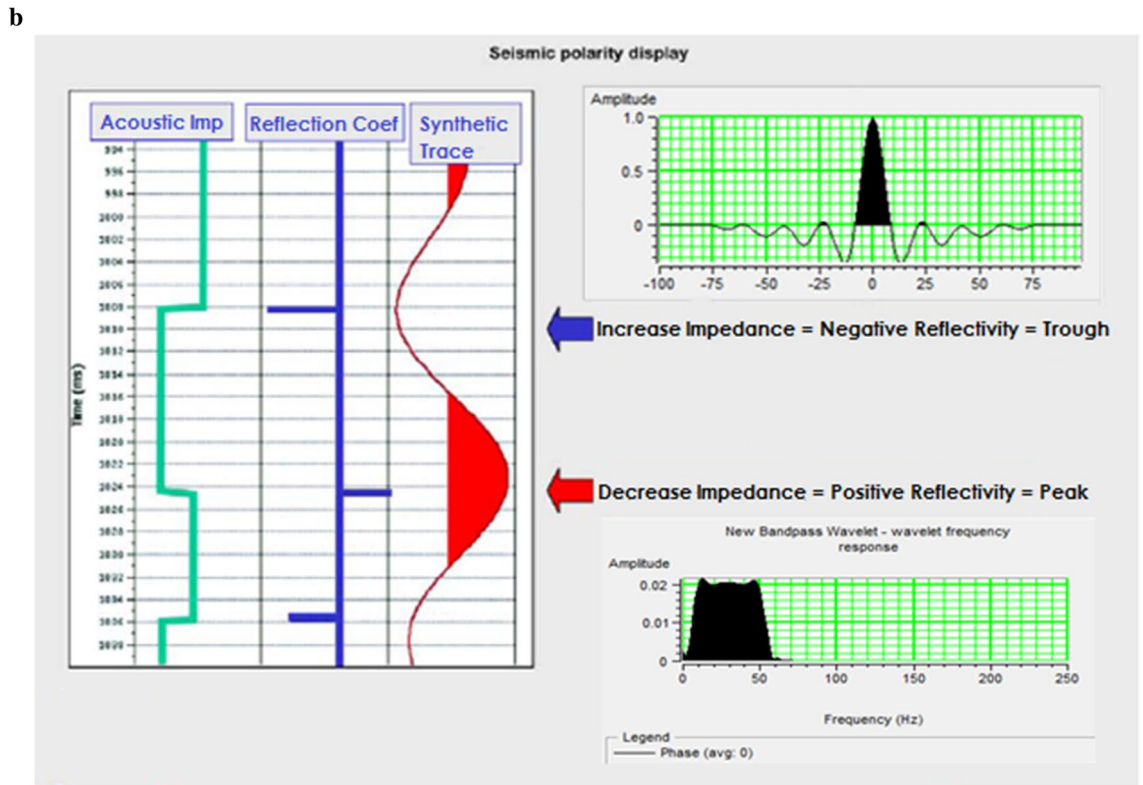
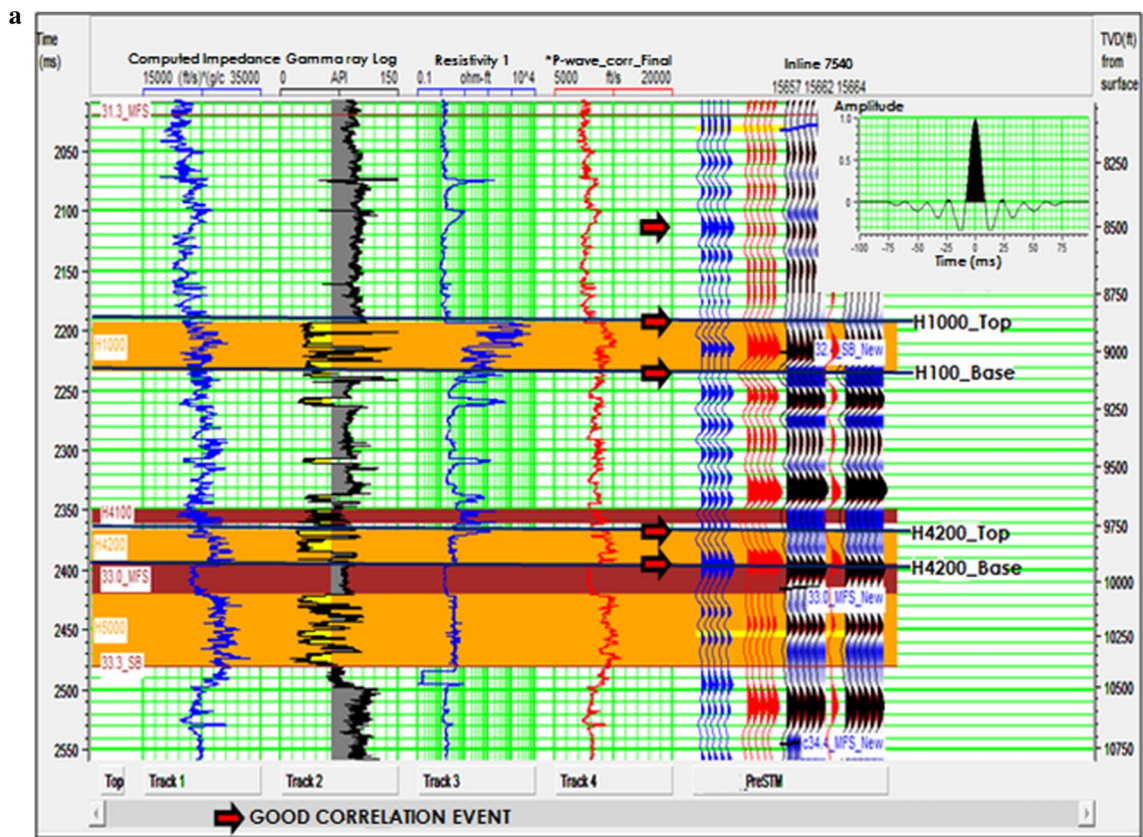


Fig. 7 a Well to seismic section showing synthetic matching with H1 reservoir TOP (as H1000_Top) and BASE (as H1000_Base) as trough event. Insert: extracted zero phased wavelet. **b** European polarity display, whereby

an increase in acoustic impedance is represented by an excursion to the left (trough) of the seismic loop. Insert: zero-phase wavelet time response at an interval of -15 to +15 ms, frequency and amplitude band response at 5–60 Hz

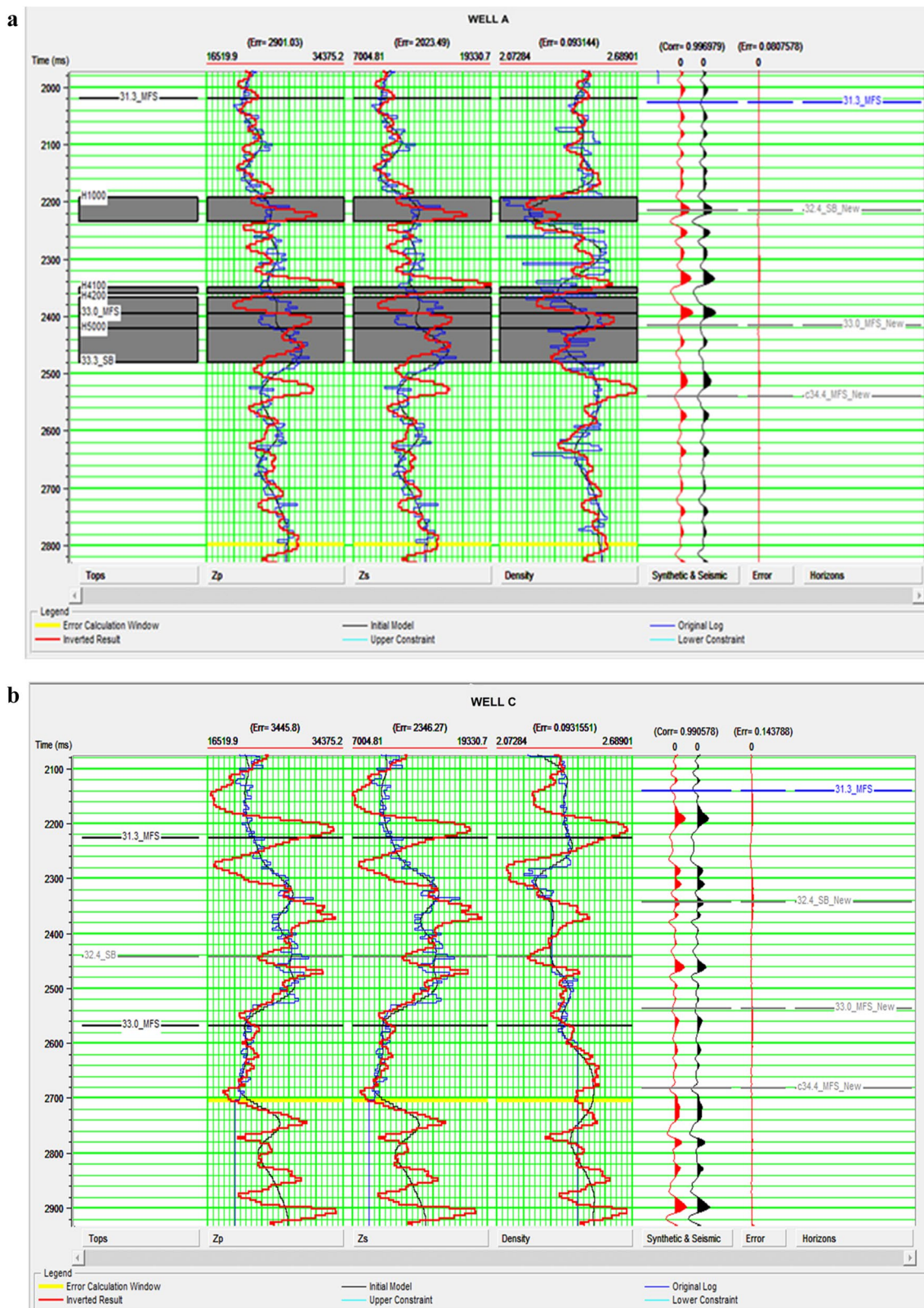


Fig. 8 a Inversion analysis result showing correlation value of 0.996979 with synthetic, seismic and picked horizons after seismic upscaling in well A. **b** Inversion analysis result showing correlation

value of 0.990578 with synthetic, seismic and picked horizons after seismic upscaling in well C

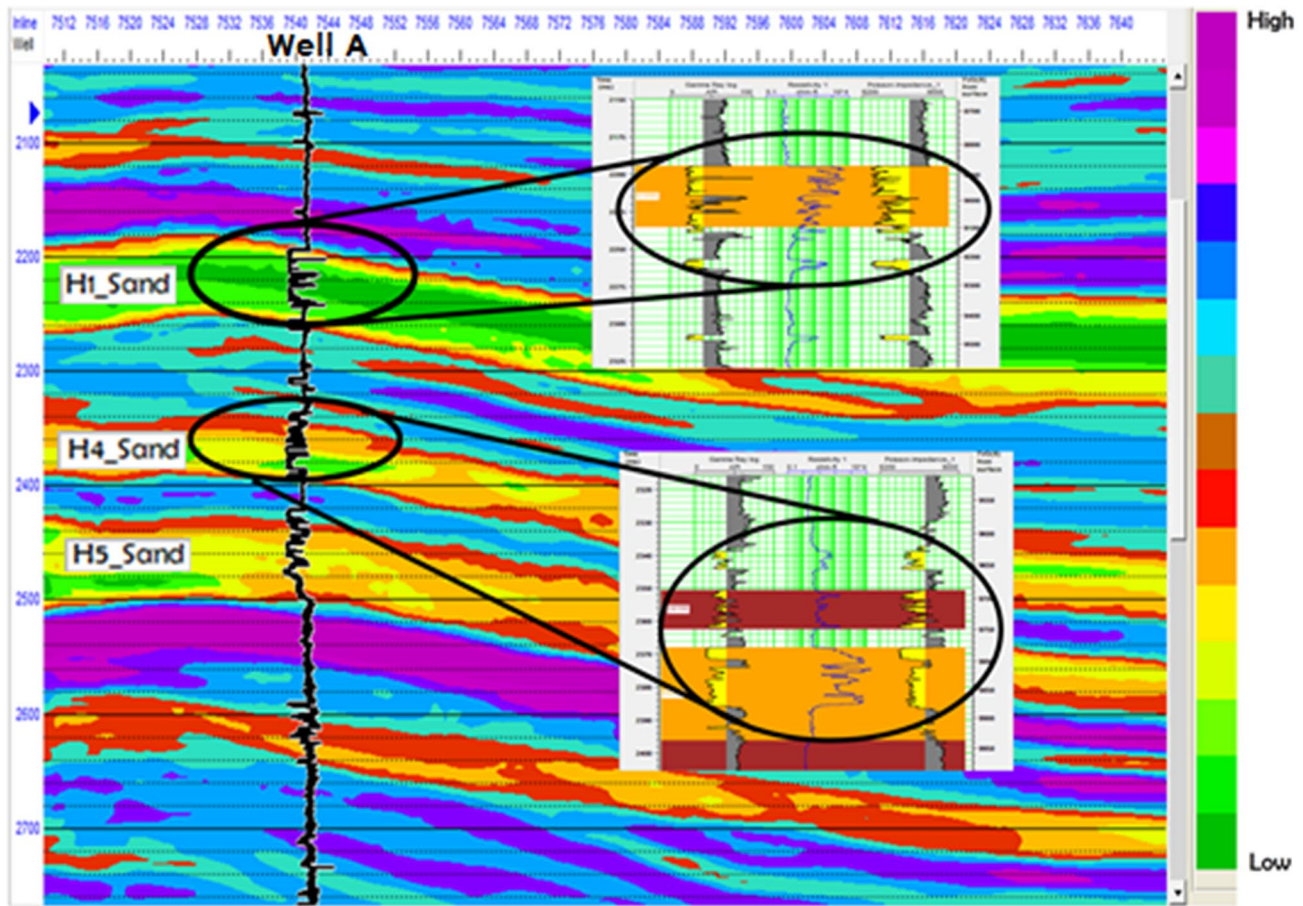


Fig. 9 Crossline section showing inverted Poisson impedance with gamma ray log (insert) over H1, H4 and H5_sands around well A. Note: low values of Poisson impedance correspond to good-quality hydrocarbon sand

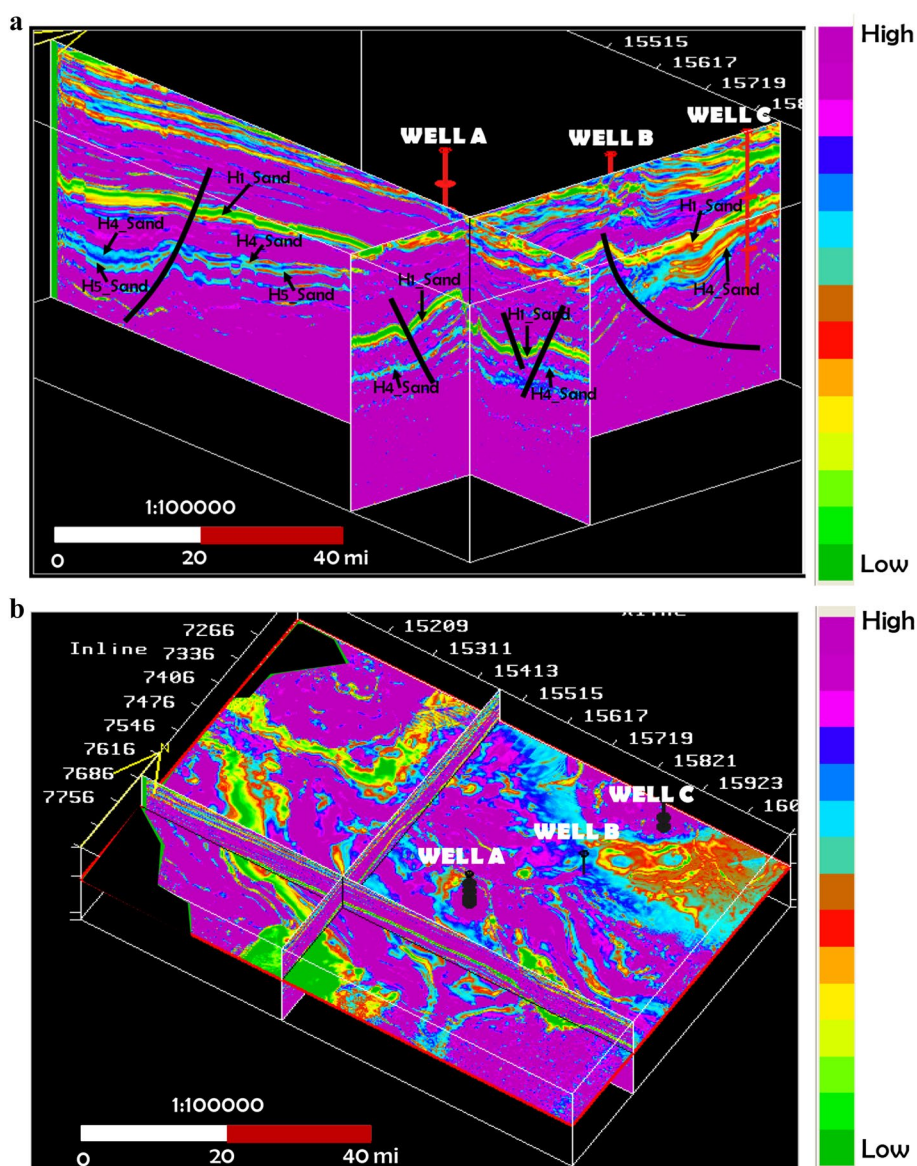
original curve of the inverted acoustic impedance (Z_p) and shear impedance (Z_s) especially at some interval (Fig. 8). Although this did not affect the inversion result the error estimate between the density, ρ , synthetic and seismic traces remains approximately zero. The practical fact behind the observed zero error is that the inversion algorithm has created impedance trace that is consistent with the wavelet and the input seismic trace.

Result from inversion modeling shows that low values of Poisson impedance reflects hydrocarbon-bearing reservoir, while medium to high value represents water (brine) and shale, respectively. On the inverted section, the H1_sand was observed to be hydrocarbon filled, with H4_sand containing brine, and hydrocarbon and H5_sands containing brine only (Fig. 9). Meanwhile, the classification of lithofacies into sand, sandy-shale, shaly-sand and shale combined with the resistivity log made the calibration for fluid types easy to understand and predict in the studied field. In Fig. 10a,

the hydrocarbon-filled H1_sand was observed to be laterally continuous even though sedimentation was mainly influenced by the west–north–west to east–south–east (WNW–ESE) trending macrostructure (Fig. 1) which was developed between 34.0 and 29.3 Ma. Observation showed that at well C (basinward), the lithofacies gradually changes from clean hydrocarbon-filled sand to sandy-shale compositions, even though they contain significant amount of hydrocarbon.

Observations based on time slice generated at 2650 ms show that hydrocarbon-filled reservoirs were mainly distributed along a northeast–southwest trending meandering channel that is away from the drilled wells (Fig. 10b). The implication is that since drilled wells (A and C) did not penetrate the hydrocarbon-filled sands, the probability of drilling more marginal or dry wells is high unless a concise depositional model is developed to validate the already known structural trappings in the field.

Fig. 10 **a** An interception (inline and crossline) section showing the distribution of faults and H-sands in the field. Note: low values of lithology impedance correspond to good-quality hydrocarbon sand. **b** A map (with inline and crossline) section at 2650 ms showing the hydrocarbon-filled channel sand in the northeast–southwest direction. Note: low values of Poisson impedance correspond to good-quality hydrocarbon sand



Conclusions

Poisson impedance (PI) inversion was applied in this study to describe an alternative technique to discriminate lithofacies and predict fluid types in the Eastern Niger Delta basin. The approach takes only the acoustic and shear impedances (Z_p and Z_s) into consideration; it is relatively simple and can be adapted in other fields in the Niger Delta Basin with regular sedimentation and tectonic activities. Four categories of lithofacies type (clean sand, sandy-shale, shaly-sand and shale) have been discriminated based on the well log cross-plot between gamma ray and Poisson impedance. The cross-plot revealed clearly very good-quality sand (sand zone), good quality (sandy-shale zone), and poor-quality sands (shaly-sand zone) from shale. Poisson impedance values obtained from the application of prestack simultaneous

inversion show those values with less than $-100 \text{ ft}^2/\text{s}^2/\text{g}/\text{cc}$ (low) as representing hydrocarbon-filled sand, whereas greater values (medium and high) represent brine and shale. The result shows that these value ranges are roughly in an acceptable agreement with the gamma ray values used for discriminating lithofacies. The validation of this technique in 3-D space revealed that the distribution of hydrocarbon-filled reservoirs was mainly distributed along a northeast–southwest trending meandering channel and that most drilled wells possibly did not penetrate the hydrocarbon-filled sands, thus leading to abandonment of wells as marginal or dry wells. Presently, exploration programs in some fields in Niger Delta basin are more commonly designed to reduce cost and increase exploration success rate so that the number of dry wells and drilling risks may be decreased if well calibrated. Finally, the methodology presented in the

paper has both a cognitive and practical aspect since it is essential for locating new sites for the drilling of new in-fill wells in areas without well control.

Acknowledgements The authors gratefully acknowledge the Shell Petroleum Development Company SPDC, Port Harcourt, Nigeria, for providing the dataset used for this study during Doctoral Research Internship program, and Petroleum Technology Development Fund (PTDF) Chair of Petroleum Geology, University of Nigeria, Nsukka, Nigeria, for the support and enabling environment for this study.

Open Access This article is distributed under the terms of the Creative Commons Attribution 4.0 International License (<http://creativecommons.org/licenses/by/4.0/>), which permits unrestricted use, distribution, and reproduction in any medium, provided you give appropriate credit to the original author(s) and the source, provide a link to the Creative Commons license, and indicate if changes were made.

References

- Aki K, Richards PG (1980) Quantitative seismology: theory and methods: W. H. Freeman and Co., New York
- Coulon JP, Lafet Y, Deschuzaux B, Doyen PM, Duboz P (2006) Stratigraphic elastic inversion for seismic Lithology discrimination in a Turbiditic Reservoir, SEG Extended Abstract, pp 2092–2096
- Doust H, Omatsola E (1989) Niger Delta. *Am Assoc Pet Geol Bull* 48:201–238
- Doust H, Omatsola E (1990) Niger Delta. In: Edwards JD, Santogrossi PA (eds) Divergent/passive margin basins, AAPG memoir 48. American Association of Petroleum Geologists, Tulsa, pp 239–248
- Duboz P, Lafet Y, Mougénot D (1998) Moving to a layered impedance cube: advantages of 3D stratigraphic inversion. *First Break* 16(9):311–318
- Ekwe AC, Onuoha KM, Osanyande N (2012) Fluid and lithology discrimination using rock physics modeling and Lambda-Mu-Rho inversion: an example from onshore Niger Delta, Nigeria. *Search and discovery article #40865*, pp 11
- Evamy BD, Haremboure J, Kamerling P, Knaap WA, Molloy FA, Rowlands PH (1978) Hydrocarbon habitat of Tertiary Niger Delta. *Am Assoc Pet Geol Bull* 62:277–298
- Farfour M, Yoon WJ, Kim J (2015) Seismic attributes and acoustic impedance inversion in interpretation of complex hydrocarbon reservoirs. *J Appl Geophys* 114:68–80
- Fatti JL, Smith GC, Vail PJ, Strauss PJ, Levitt PR (1994) Detection of gas in sandstone reservoirs using AVO analysis: a 3-D seismic case history using the Geostack technique. *Geophysics* 59:1362–1376
- Goodway B, Chen T, Downton J (1997) Improved AVO fluid detection and lithology discrimination using Lamé petrophysical parameters: $\lambda\rho$, $\mu\rho$, & λ/μ fluid stack, from P and S inversions: 67th annual international meeting, SEG, Expanded Abstracts, pp 183–186
- Hampson DP, Russell BH, Bankhead B (2005) Simultaneous inversion of pre-stack seismic data, 75th SEG Meetings, SEG Expanded Abstracts, pp 1633–1636
- Lawrence SR, Monday S, Bray R (2002) Regional geology and geophysics of the eastern Gulf of Guinea (Niger Delta to Rio Muni). *Lead Edge* 21:1112–1117
- Ma XQ (2002) Simultaneous inversion of Prestack seismic data for rock properties using simulated annealing. *Geophysics* 67:1877–1885. <https://doi.org/10.1190/1.1527087>
- Mazumdar P (2007) Poisson damping factor. *Lead Edge* 26:850–851. <https://doi.org/10.1190/1.2756862>
- Nair KN, Kolbjørnsen O, Skorstad A (2012) Seismic inversion and its applications in reservoir characterization. *First Break* 30:83–86
- Nwogbo PO, Omudu M, Dike R, Olotu S, Osayande N (2009) Seismic-based lithology and fluid delineation of the ROK reservoir sand, shallow offshore Niger Delta. In: SEG Technical Program Expanded Abstracts 2009, pp 608–612. <https://doi.org/10.1190/1.3255830>
- Omudu LM, Ebeniro JO, Xynogalas M, Adesanya O, Osayande N (2007) Beyond acoustic impedance: an onshore Niger Delta experience. In: SEG/San Antonio Annual Meeting, pp 412–415
- Orife JM, Afbovo AA (1981) Stratigraphic and unconformity traps in the Niger delta—Abstract. *Am Assoc Pet Geol Bull* 65:251–265
- Petters SW (1984) An ancient submarine canyon in the Oligocene-Miocene of the western Niger Delta. *Sedimentology* 31:805–810
- Quakenbush M, Shang B, Tuttle C (2006) Poisson impedance. *Lead Edge* 25(2):128–138. <https://doi.org/10.1190/1.2172301>
- Reijers TJA (2011) Stratigraphy and sedimentology of the Niger-Delta. *Geologos* 17(3):133–162
- Reijers T, Petters S, Nwajide C (1997). In: Selley RC (ed) *The Niger Delta Basin, African Basins—Sedimentary Basin of the World* 3. Elsevier Science, Amsterdam, pp 151–172
- Russell BA (2014) Prestack seismic amplitude analysis: an integrated overview. *Interpretation* 2(2):SC19–SC36. <https://doi.org/10.1190/INT-2013-0122.1>
- Sen MK (2006) Seismic inversion. Society of Petroleum Engineers (SPE), pp 120. ISBN: 978-1-55563-110-9
- Sharma RK, Chopra S (2013) Poisson impedance inversion for characterization of sandstone reservoirs, SEG/Houston Annual Meeting, pp 2549–2553. <https://doi.org/10.1190/segam2013-0181.1>
- Short KC, Stauble AJ (1967) Outline of geology of Niger Delta. *Am Asso Petrol Geol Bull* 51:761–779
- Singh V, Srivastava AK, Painuly PK (2007) Neural networks and their applications in lithostratigraphic interpretation of seismic data for reservoir characterization. *Lead Edge* 26(10):1244–1260
- Singleton SW (2011) The effects of seismic data conditioning on pre-stack simultaneous impedance inversion: GCSSEPM 31st Annual Bob. F. Perkins Research Conference, pp 35–65
- SPDC Internal Report (2007) Onshore to deep water geologic integration, Niger Delta. In: Ejedawa J, Love F, Steele D, Ladipo K (eds) Presentation packs of Shell Exploration and Production Limited, Port-Harcourt (unpublished)
- Stacher P (1995) Present understanding of the Niger Delta hydrocarbon habitat. In: Oti MN, Postma G (eds) *Geology of Deltas*. A.A. Balkema, Rotterdam, pp 257–267
- Tian L, Zhou D, Lin G, Jiang L (2010) Reservoir prediction using Poisson Impedance in Quinhuangdao, Bohai Sea: SEG Denver 2010 Annual Meeting, pp 2261–2264
- Tucovic N, Bartetzko A, Wessling S, Schön J, Gegenhuber N (2016) Resistivity and acoustic impedance based rock physics templates for enhanced well placement and reservoir understanding. In: 78th EAGE conference and exhibition, extended abstracts, We STZ013
- Ujuanbi O, Okolie JC, Jegede SI (2008) Lambda-Mu-Rho techniques as a viable tool for litho-fluid discrimination. *The Niger Delta example*. *Int J Phys Sci* 2/7:173–176
- Veeken PC, Da Silva M (2004) Seismic inversion methods and some of their constraints. *First Break* 22(6):47–70
- Wang Y (1999) Simultaneous inversion for model geometry and elastic parameters. *Geophysics* 64:182–190
- Whiteman A (1982) Nigeria: its petroleum geology, resources and potential. Graham and Trotman, London, pp 394
- Zhou ZY, Hilterman FJ (2010) A comparison between methods that discriminate fluid content in unconsolidated sandstone reservoirs. *Geophysics* 75(1):B47–B58. <https://doi.org/10.1190/1.3253153>

Publisher's Note Springer Nature remains neutral with regard to jurisdictional claims in published maps and institutional affiliations